

# STUDY OF HYBRID DRY COOLING SYSTEMS FOR STE PLANTS BASED ON LATENT STORAGE

Rocío Bayón<sup>1\*</sup>, Mario Biencinto<sup>1</sup>, Esther Rojas<sup>1</sup>, Nerea Uranga<sup>2</sup>

CIEMAT-PSA<sup>1</sup>

Av. Complutense 40, 28040 Madrid, Spain.

Phone: +34 913466048

IK4-TEKNIKER<sup>2</sup>

C/ Iñaki Goenaga 5, 20600 Eibar, Guipuzkoa, Spain

E-Mail: [rocio.bayon@ciemat.es](mailto:rocio.bayon@ciemat.es)

5

## 10 1 SUMMARY

This work focuses on the study of a hybrid cooling system for a solar thermal electricity (STE) plant composed by a latent storage module and an air-cooled condenser. In a first approach various commercial products have been studied in order to determine their feasibility as PCMs for the latent storage module. Differential scanning calorimetry (DSC), heat capacity ( $C_p$ ) measurements and daily thermal cycling tests have been performed in order to determine the thermal properties of the selected PCMs and their melting/freezing behavior. Form these tests the product RT35HC has been chosen as PCM for the latent module. In order to evaluate the advantage of using a hybrid versus a conventional dry cooling system, the annual performance in terms of electricity production of a STE plant located in Ouarzazate (Morocco) has been simulated with both kinds of systems. Simulation results show that 0.31% increase in electricity could be obtained per year if a hybrid cooling system was used. However, the feasibility of this concept strongly depends on economic issues like electricity prices along the plant lifetime and both materials and equipment cost for the latent storage system.

15

20

## 2 INTRODUCTION

A Solar Thermal Electricity (STE) plant, as any other thermal power plant, requires large amounts of water (from 2000 to 3000 m<sup>3</sup>/GWh) for its operation and maintenance. The majority of this water, about 82% to 94%, is consumed in power-block cooling whereas the rest is used for steam generation and solar field cleaning. Taking into account that areas with high direct solar irradiation and hence most appropriate for STE plants may be deserts with low water availability, the implementation of water saving strategies in a power plant to be constructed in those locations is major issue. The WASCOP project aims to overcome such challenge by offering different solutions for reducing water consumption in STE plants. Some of the water saving strategies included in WASCOP project are focused on the power-block cooling system since, as said above, a high percentage of water consumption in these plants is devoted to it. The Task 2.2 of this project evaluates the feasibility of a dry cooling concept, initially proposed by Pistocchini and Motta, 2011. This concept consists on using an air-cooled condenser (ACC) combined with a latent storage module as a hybrid cooling system. The latent module accumulates all or part of the exhaust heat from the turbine during the day for releasing it during the night, when lower ambient temperatures are expected. This should not only reduce ACC fan power consumptions but also improve the overall performance of the power block. With this approach, the condensation temperature during turbine operation can be maintained in most cases at lower values than with a conventional ACC cooling system and hence the efficiency of the power cycle can be increased. The heat stored in the latent module is released to the environment at night-time with the help of the ACC by taking advantage of the lower ambient temperature. The selection of the most adequate phase change material (PCM) to be implemented in the latent storage module has to take into account both the temperature of the exhaust heat released by the power block and the ambient conditions of the locations in which the STE plant may be constructed. These requirements impose that PCM should have a phase change temperature in the range of 25 °C to 40 °C.

25

30

35

40

45 In this work some commercial PCMs have been considered in order to ensure their availability in the market  
 and also with the hope that problems related to material stability are already solved by the manufacturer. Prior  
 to selecting the most appropriate PCM, the thermal properties required for the storage module design were  
 measured for the selected candidates. Also, daily melting/freezing cycles under air were performed in a  
 50 temperature controlled oven in order to study the PCMs under conditions similar to the operating ones and  
 hence assessing their feasibility as storage materials for this specific application.

After selecting one PCM, annual simulations of performance for a typical STE plant located in a deserted  
 location with this kind of cooling system have been carried out. Similar simulations have been done for the  
 same STE plant with a conventional ACC cooling system and the results have been compared and discussed.

### 3 EXPERIMENTAL

55 In this work four commercial PCMs, two organic (RT35HC and RT28HC) and two inorganic (SP31 and  
 SP26E), were tested since this manufacturer can supply small amounts of materials (1 kg) and also offers the  
 possibility of PCM encapsulation, which would facilitate product handling, especially because melting  
 temperatures are too close to room temperature. The thermophysical properties of these PCMs provided by the  
 manufacturer (Rubitherm, 2017) are recorded in Table 1.

60 Table 1: Thermophysical properties of PCMs tested (Rubitherm, 2017).

Product	Type	$T_{\text{melt}}$ ( $^{\circ}\text{C}$ )	$\Delta H_{\text{melt}}$ (kJ/kg)	$\rho$ (kg/m <sup>3</sup> )	k(W/mK)	$T_{\text{max}}$ ( $^{\circ}\text{C}$ )
RT35HC	Organic	35	240	860 (s)	0.2	70
				770 (l)		
SP31	Inorganic	31-33	220	1350 (s)		60
				1300 (l)		
RT28HC	Organic	28	245	880 (s)	0.2	50
				770 (l)		
SP26E	Inorganic	25-27	190	1500 (s)	0.6	60
				1400 (l)		

Thermal characterization of these PCMs was performed by using a Mettler Toledo DSC1/500 apparatus.  
 Temperature was calibrated with both In and Zn standards and enthalpy was verified with the In standard. DSC  
 scans for obtaining phase change enthalpies and temperatures ( $T_{\text{melt}}$ ,  $\Delta H_{\text{melt}}$ ) were carried out at 10 $^{\circ}\text{C}/\text{min}$ ,  
 65 under N<sub>2</sub> flux at 50ml/min and samples were contained inside 40 $\mu\text{l}$  aluminium crucibles with micro-perforated  
 covers. Heat capacity ( $C_p$ ) measurements were performed in the same DSC apparatus under similar  
 experimental conditions in terms of calibration standards, N<sub>2</sub> flux and sample containers. However, the specific  
 method for obtaining  $C_p$  implies to perform a base line, then a calibration with a sapphire standard and finally  
 the measurement of the corresponding sample. This measurement consisted in two 10 min isothermal steps at  
 70 both minimum and maximum temperature and a dynamic test at 10  $^{\circ}\text{C}/\text{min}$ .

In order to prove the viability of these PCMs as storage materials, tests under conditions as close as possible to  
 the service ones should be required. In this way daily heating/cooling cycles were performed in an oven under  
 air for samples of about 4-30 g contained in a ceramic crucible. Temperature interval and heating/cooling rate  
 depended on the kind of PCM tested. During the cycles, sample temperature was monitored for detecting any  
 75 change in PCM behaviour.

## 4 PCM CHARACTERIZATION

### 4.1 DSC measurements

80 DSC scans for the organic PCMs (RT35HC and RT28HC) were performed twice in order to homogenize the samples. The curves corresponding to the second heating/cooling cycle are displayed in Fig. 1. As we can see, none of these PCMs shows supercooling although during freezing they show two transitions. For RT35HC the two transitions are clearly distinguished whereas for RT28HC they are not so good resolved and only a shoulder is observed. However, if cooling rate was lower, probably two peaks would probably be obtained as well. For both materials phase change temperatures agree quite well with the values recorded in Table 1, however enthalpies are higher than the ones provided by the manufacturer (see Table 1), especially for RT35HC. Soupart-Caron, 2015, also performed DSC measurements and obtained phase change enthalpies around 234 kJ/kg and hence also higher than the value given by the manufacturer (see Table 1).  
85

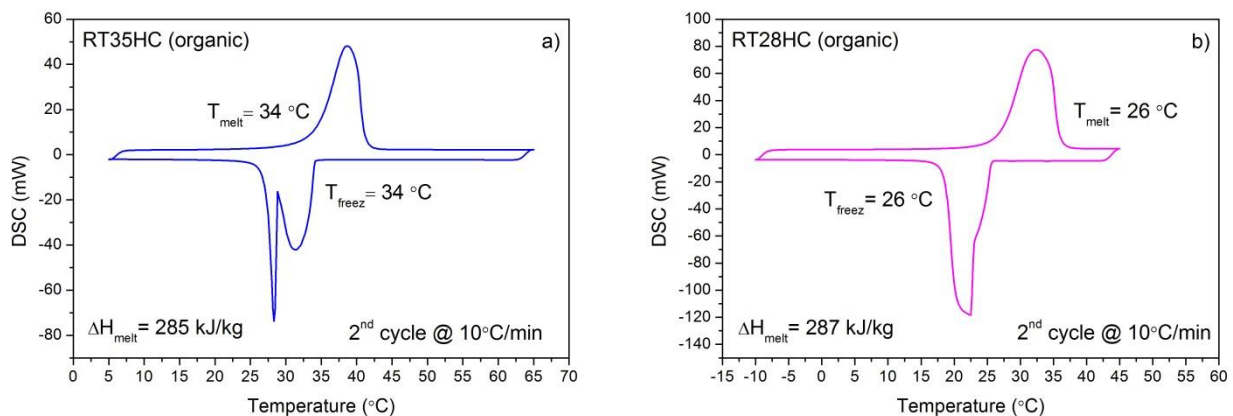


Fig. 1: DSC measurements performed for the organic PCMs RB35HC a) and RB28HC b).

90 When DSC measurements were performed for the inorganic PCMs (SP31 and SP26E), which are hydrated salts, some problems were encountered. For the case of RT31SP the initially solid sample was heated at  $10\text{ }^{\circ}\text{C/min}$  and a melting peak at  $34\text{ }^{\circ}\text{C}$  was observed with an enthalpy of  $277\text{ kJ/kg}$ . However, when this sample was cooled down, no freezing peak was observed even if a final temperature of  $-40\text{ }^{\circ}\text{C}$  was attained. Therefore, a second sample was prepared but this time SP31 was initially in liquid estate. This time DSC measurements  
95 were performed at  $0.5\text{ }^{\circ}\text{C/min}$  starting with a cooling cycle down to  $-25\text{ }^{\circ}\text{C}$  and a subsequent heating run up to  $55\text{ }^{\circ}\text{C}$ . These cycles are displayed in Fig. 2 a) and, as we can see, both melting and freezing peaks are observed at  $26\text{ }^{\circ}\text{C}$  and  $17\text{ }^{\circ}\text{C}$  respectively. However the enthalpies obtained in these runs are about  $37\text{ kJ/kg}$  and hence much lower than the value reported by the manufacturer.

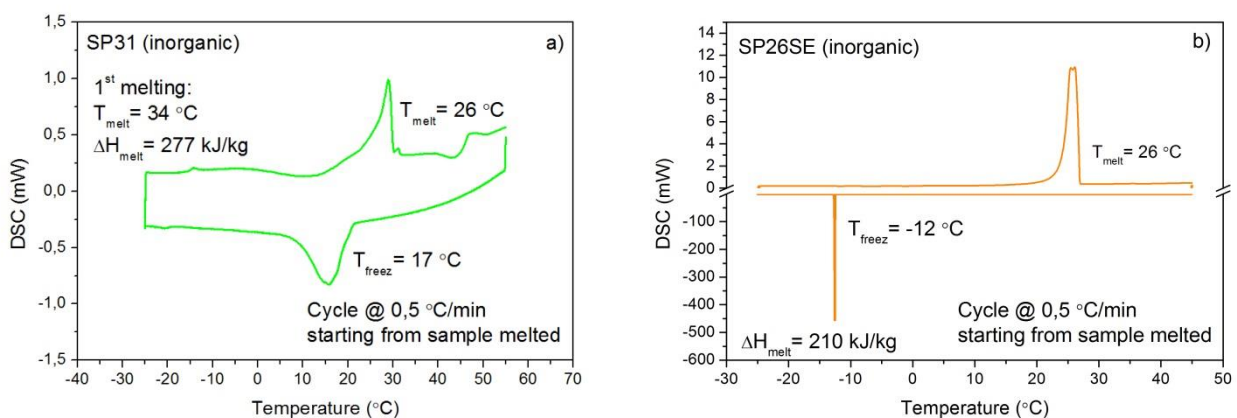
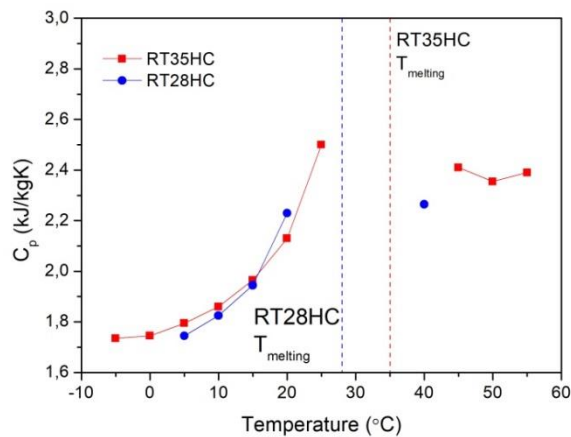


Fig. 2: DSC measurements performed for the inorganic PCMs SP31 a) and SP26E b).

The other inorganic PCM (SP26E) shows a better behavior in DSC scans with quite a high enthalpy, but it has a strong supercooling since it melts at 26 °C but it does not solidify until temperature reaches -12 °C (see Fig. 2 (b)). Apart from supercooling the reason for the behavior of these inorganic PCMs (hydrated salts) can be due to the occurrence of incongruent melting/freezing phenomena.

## 105 4.2 $C_p$ measurements

In general,  $C_p$  measurements are much more difficult to perform than DSC scans since they are not so straight forward. Actually,  $C_p$  values for the inorganic PCMs (SP31 and SP26E), which displayed strong supercooling and maybe incongruent melting/freezing, could not be carried out by applying the conventional methods developed in the laboratory for such measurements. Only the organic PCMs (RT35HC and RT28HC) could be measured and the variation of  $C_p$  with temperature was obtained, as displayed in Fig. 3. For both PCMs we observe that in solid state increases  $C_p$  as temperature approaches the melting point and it shows a constant value afterwards.  $C_p$  values given by the supplier for both PCMs are 2 kJ/kgK (see Table 1), which is the mean value we observe for the solid phase of these two PCMs. However, as displayed in Figure 3, in liquid state they show slightly higher values of around 2.2-2.3 kJ/kgK.



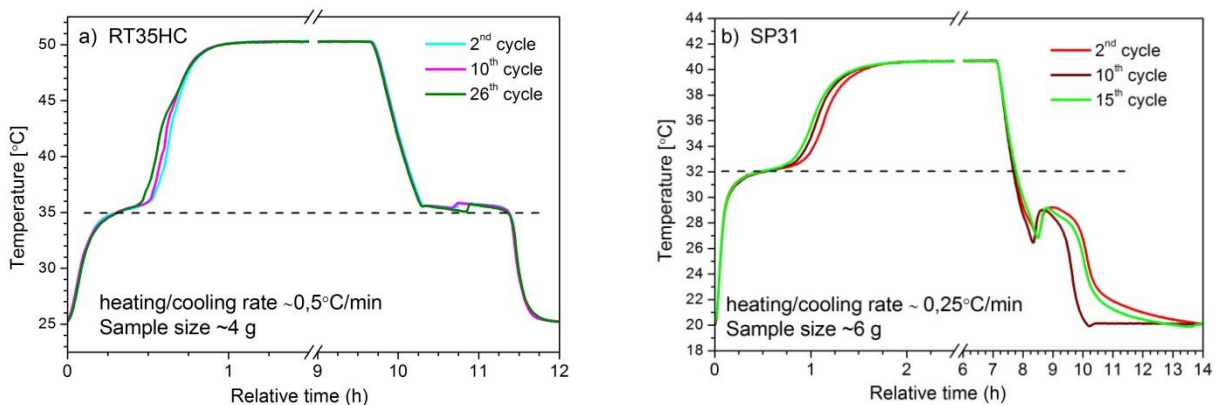
115

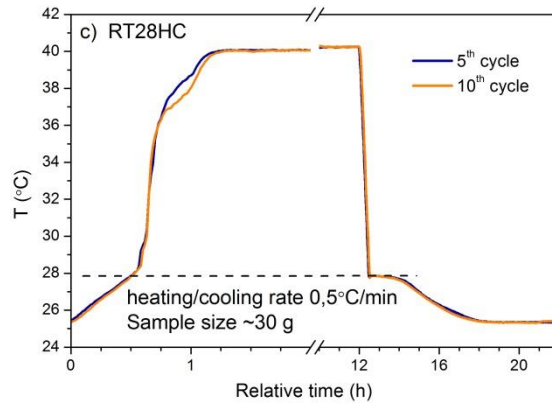
Fig. 3:  $C_p$  measurements performed for the organic PCMs: RB35HC and RB28HC

## 4.3 Daily heating/cooling cycles

Daily heating/cooling cycles were performed for the selected commercial PCMs in order to reproduce test conditions closer to the service conditions in comparison with DSC measurements. Temperature interval for the cycles was  $\pm 10$ -20 °C around  $T_{melt}$  taking care that working temperature limit recommended by the manufacturer (see Table 1) was not exceeded. In Fig. 4 temperature-time curves for RT35HC a), SP31 b) and RT28HC c) are recorded and the curves corresponding to different cycles are compared.

120





125 Fig. 4: Temperature-time curves of daily heating/cooling cycles performed in the oven under air for RT35HC  
 a), SP31 b) and RT28HC c).

For the three PCMs tested the temperature-time curves remain almost the same not only for the first cycles (2<sup>nd</sup> and 5<sup>th</sup>) but also for the last cycles performed (10<sup>th</sup>, 15<sup>th</sup> or 26<sup>th</sup>). In this kind of tests a flat plateau should be observed during both heating and cooling processes around melting temperature. RT35HC behaves this way not only in the 2<sup>nd</sup> cycle but also in the 26<sup>th</sup> cycle. RT31SP also displays a plateau during heating around melting temperature, whereas during cooling, temperature has to go down to 26 °C until solidification occurs, which means that this compound presents supercooling. The latent heat produced during the freezing is able to heat up the sample and this is why the temperature-time curve has this shape. SP31 behaves much better when cycled in the oven than in DSC measurements (see Fig. 2 (left)). In oven test this SP31 also displays supercooling, but the extent of this phenomenon is smaller since for this test a sample of about 5 g was used in comparison to the sample sizes used in DSC measurements which are normally in the order of 10-20 mg. This shows the importance of performing heating/cooling tests for PCMs under conditions as similar as possible to the service ones. RB28HC does not display a flat plateau during heating but a slope ending at  $T_{\text{melt}}=28$  °C. However, it does show a plateau during cooling at this temperature. Finally, SP26 could not be tested since lab temperature is practically the same as melting temperature which makes it difficult the testing of this PCM even in an oven with forced ventilation. Moreover, if we take into account DSC results, some supercooling should be expected which means that freezing temperature would be lower than 26 °C.

135  
 140 Taking into account both DSC results and cycling test in the oven we can say that the RT35HC is the most reliable of the three commercial PCMs tested for being implemented in the latent storage module of the hybrid cooling system.  
 145

## 5 IMPLEMENTATION OF THE LATENT STORAGE MODULE IN THE DRY COOLING SYSTEM

For implementing a latent storage module in a hybrid dry cooling system of a STE plant, similar to the one proposed by Pistocchini and Motta, 2011, it is necessary to establish the operating conditions of the plant and this will depend on its geographical location. The chosen STE plant is a conventional one with a 55 MW<sub>e</sub> gross rated power block, a solar field of parabolic troughs with thermal oil as heat transfer fluid and 2-tank molten-salt thermal storage of 8 h capacity. A STE plant of this kind in a good summer day is expected to operate about 12 h with solar-only support plus 8 h from the storage system, which implies 20 h operation of the power block. This leaves a window of 4 h for discharging the latent storage system because, for simplicity, we assume that discharging process should take place when turbine is not under operation. Therefore, we have chosen 3 h for the latent storage capacity for which we can arrange charging and discharging processes whenever it is convenient.  
 150  
 155

Taking into account that RT35HC displays a good thermal behavior, we chose this PCM for a preliminary design of a hybrid dry cooling system for a STE plant that includes an air-cooled condenser (ACC) combined



with a latent storage module. In Fig. 5 the scheme of such dry cooling system in a direct configuration is displayed for both charging (a) and discharging processes (b). During charging process, exhaust heat from turbine output is delivered to the latent storage and/or to the ACC by means of a three-way control valve, depending on ambient temperature and latent storage state. Due to the melting temperature of the PCM and considering a pinch point of 3 °C, the temperature of the exhaust steam leaving the turbine outlet should be, at least, 38 °C (0.0663 bar condensing pressure). Therefore, this would be the minimum charging temperature for the latent storage module.

a) Charging process

b) Discharging process

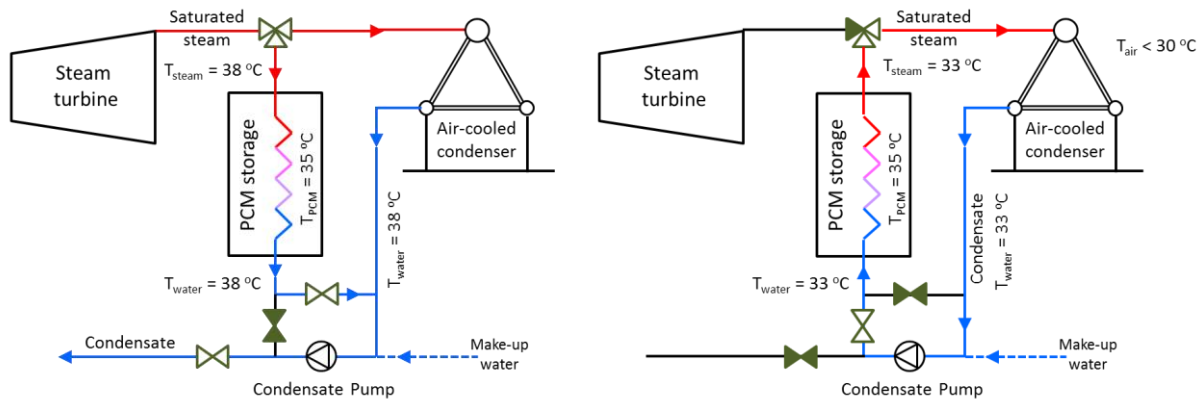


Fig. 5: Schemes of charging (a) and discharging (b) processes of a direct cooling system for a STE plant that combines a latent storage module with an air-cooled condenser.

During the night-time, when steam turbine is not working, latent storage can be discharged by producing low temperature steam which is condensed with the help of the ACC. Hence, for discharge processes 2 °C pinch point is assumed in the latent storage module and at least an additional pinch point of 3 °C in the ACC has to be considered as well. This implies that the ambient temperature required to condense the steam coming from the storage should be well below 30 °C.

### 5.1 Daily heating/cooling cycles of RT35HC between real operating temperatures

From the schemes of Fig. 5 it is clear that the latent storage containing RT35HC will be charged and discharged at 38 °C and 33 °C respectively. This means that this PCM should be able to melt and freeze completely within such a narrow temperature range (5 °C). In order to study RT35HC behavior under these conditions additionally daily heating/cooling cycles were performed in the temperature intervals 38 °C-33 °C and 37 °C-34 °C. The resulting temperature-time curves for both the sample are displayed in Fig. 6. The plots show that RT35HC undergoes melting not only when oven temperature is 3 °C above  $T_{melt}$  but also when it is 2 °C above, since in both cases a shoulder is observed. Obviously, the lower the temperature gradient inside the oven the slower the melting process is. Actually, if we compare with the temperature-time curves of Fig. 4 a), for which oven temperature is 50° C, we can see that the melting process is faster for the same amount of sample (4 g). Note that time scales of Fig. 4 a) and Fig. 5 are different. Sample state (either liquid or solid) was checked by visual inspection with a quick open-close of the oven. We could assess that PCM was completely melted when the flat constant temperature segment was attained (either 38 °C or 37 °C) and that it was completely solid during the flat segments at 34 °C and 33 °C.

These results prove that RT35HC undergoes full phase change even within a very narrow temperature interval ( $T_{melt} \pm 2\text{ °C}$ ) although we have to take into account that melting/freezing time could be long and hence storage power could be lower than expected.

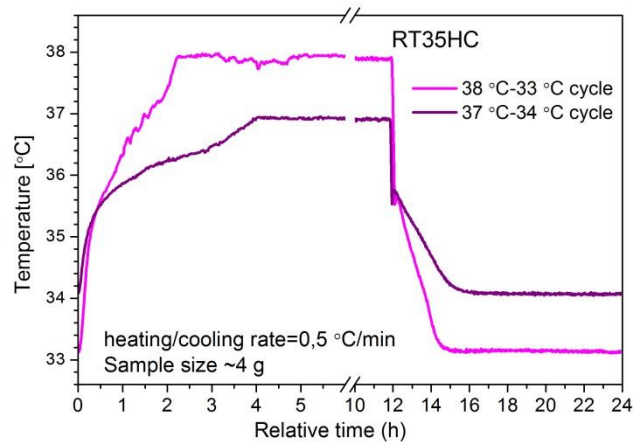


Fig. 6: Temperature-time curves of daily heating/cooling cycles performed for RT35HC in the oven under air in the temperature intervals: 38 °C-33 °C and 37 °C-34 °C.

## 5.2 Desert selection and results of annual simulation of the STE plant

195 After evaluating the yearly ambient temperatures of various deserted locations, we chose Ouarzazate (Morocco) because it shows very high diurnal temperatures (above 35°C) and low enough night-time temperatures (down to 17°C). In Fig. 7 a) daily temperature variation in the hottest month (July) for this desert is displayed. As we can see, the most appropriate time window for discharging the latent storage is between 3 a. m. and 6 a. m. since ambient temperature is the lowest. In Fig. 7 b) the daily mean temperature of this time window for the summer months (June-September) has been plotted. In this graph we see that July and August have the highest minimum mean temperatures and for both of them a mean temperature value of about 20 °C is obtained for the whole month.

200

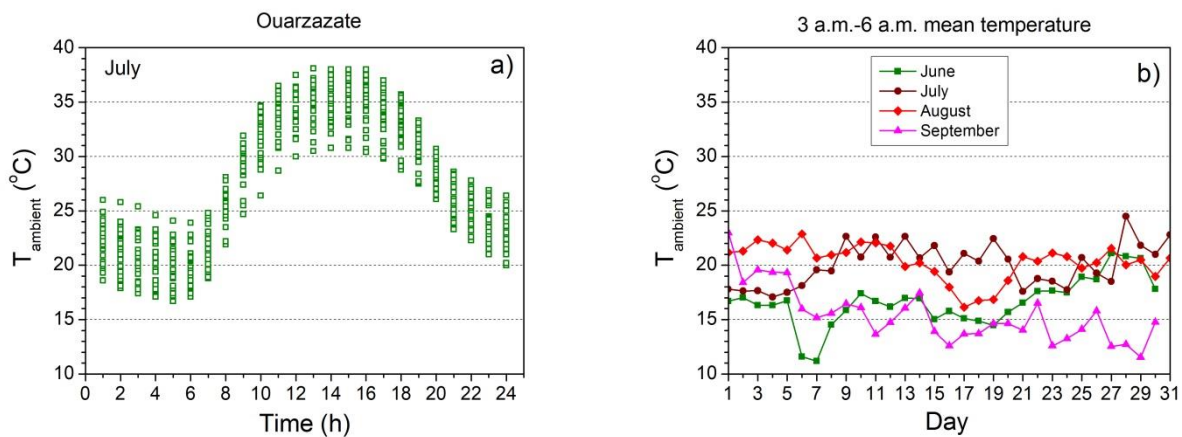


Fig. 7: Daily temperature variation in Ouarzazate (Morocco) in July (a) and mean temperature between 3 a. m. and 6 a. m. for the summer months in the same location (b).

205

The simulation model for evaluating the STE plant annual performance was developed in TRNSYS software environment (Klein et al., 2013) and is basically composed by a solar field, a thermal storage system and a power block. Nevertheless, the implementation adopted for this study allows the possibility of including either a dry cooling system based on a conventional ACC or a hybrid system that combines ACC and latent storage so that both options can be compared. An overall description of the STE plant model can be found in Biencinto et al., 2014.

210

Annual simulations of the two STE plant options mentioned above were performed by using as input file a typical meteorological year (TMY) of Ouarzazate (30.933o N, 6.9o W) provided by MASEN (MASEN, 2017).

215 For a STE plant with a conventional direct dry cooling system (only with ACC) the model yields an annual net  
electricity production of 180.35 GWh<sub>e</sub>, whereas for the plant with a hybrid cooling system (ACC combined  
with latent storage) the annual net production obtained is 180.91 GWh<sub>e</sub>. Hence by using the hybrid cooling  
system a net electricity gain of 560 MWh<sub>e</sub> is obtained. This corresponds to 0.31% of the expected annual  
220 production for the proposed STE plant in this location. Actually, the electricity production can be further  
increased if strategies for plant integration are optimized. However, we have to take into account that apart  
from the increase in annual production, the cost-effectiveness of the hybrid cooling system will strongly depend  
on both electricity prices and PCM costs.

## 6 CONCLUSIONS

225 In this work four commercial products (RT35HC, RT28HC, SP31 and SP26E) have been characterized and  
tested in order to prove their feasibility as PCMs for a latent storage module that, combined with an air-cooled  
condenser (ACC), should work as dry cooling system for a STE plant. Taking into account both DSC results  
and daily heating/cooling cycles test performed in an oven we can conclude that the RT35HC is the most  
reliable material from the original candidate list.

230 In order to evaluate the advantage of using a hybrid (latent storage+ACC) versus a conventional direct dry  
cooling, annual simulations of a STE plant located in Ouarzazate (Morocco) with either one or other system  
have been performed. For a plant in this location it has been obtained that by using a hybrid cooling system  
based on RT35HC, the expected annual electricity production can be 0.31% increased. However, the economic  
feasibility of this cooling concept will depend not only on electricity prices and PCM cost but also on the  
expected incomes along the useful lifetime of the plant, which should be able to overcome the total cost of both  
materials and equipment for the latent storage system.

235 On the other hand, although RT35HC fits temperature conditions of Ouarzazate desert, PCMs with higher  
melting temperatures might be more suitable for other deserted locations with higher night-time temperatures  
allowing higher gains in terms of electricity production.

## 7 FUNDING

240 This work has been developed thanks to the financial support of WASCOP project from H2020 Program (Grant  
agreement: 654479) and of ALCCONES Project (S2013/MAE-2985) from the Community of Madrid Program  
of R&D activities between research groups in Technologies 2013, co-financed by structural funds.

## 8 REFERENCES

- 245 Biencinto M., Bayón R., Rojas E., González L. (2014) Simulation and assessment of operation strategies for  
solar thermal power plants with a thermocline storage tank. *Sol. Energy*, 103, 456-472.  
doi:10.1016/j.solener.2014.02.037.
- Klein S.A. et al. (2013) TRNSYS 17: A Transient System Simulation Program. Solar Energy Laboratory,  
University of Wisconsin-Madison: <http://sel.me.wisc.edu/trnsys>
- MASEN: Moroccan Agency of Sustainable Energy (2017): <http://www.masen.ma/en/>
- 250 Pistocchini L., Motta M. (2011) Feasibility Study of an Innovative Dry-Cooling System With Phase-Change  
Material Storage for Concentrated Solar Power Multi-MW Size Power Plant. *ASME. J. Sol. Energy  
Eng.*,133(3), 031010-031010-8. doi:10.1115/1.4004268.
- Rubitherm web site (2017): <http://www.rubitherm.eu>
- Soupart-Caron A. (2015) Stockage de chaleur dans les matériaux à changement de phase. Génie des procédés.  
Université Grenoble Alpes, Français. <NNT : 2015GREAI078>.<tel-01266813>

255



Please fill in for the chairs:

260

Name: Rocío

Surname: Bayón

Institute, company, organisation: CIEMAT-PSA

Key activities: Thermal storage materials and systems

265

Miscellaneous: PhD in Chemistry, 20 year experience in materials for solar energy, last 10 years working in thermal storage field